In presenting the dissertation as a partial fulfillment of the requirements for an advanced degree from the Georgia Institute of Technology, I agree that the Library of the Institute shall make it available for inspection and circulation in accordance with its regulations governing materials of this type. I agree that permission to copy from, or to publish from, this dissertation may be granted by the professor under whose direction it was written, or, in his absence, by the Dean of the Graduate Division when such copying or publication is solely for scholarly purposes and does not involve potential financial gain. It is understood that any copying from, or publication of, this dissertation which involves potential financial gain will not be allowed without written permission.

_____

_____

7/25/68

DIFFUSION IN THE PRESENCE OF SEDIMENTATION

A THESIS

Presented to

The Faculty of the Division of Graduate

Studies and Research

By

David W Moore

In Partial Fulfillment

of the Requirements for the Degree

Master of Science in Chemical Engineering

Georgia Institute of Technology

October, 1972

DIFFUSION IN THE PRESENCE OF SEDIMENTATION

Approved:

Clyde Orr, Jr., Chariman

Charles W. Gorton

Jude T. Sommerfeld

Date approved by Chairman: 10-10-72

ACKNOWLEDGMENTS

My sincerest thanks are extended to Dr. Clyde Orr, Jr. for his invaluable guidance and help in completing this work. Thanks are expressed also to the staff and management of Micromeritics Instruments Corporation, Norcross, Georgia for their cooperation, especially to Susan Richardson and Jack Smithwick for their personal interest and help in my project. I would also like to thank Dr. Charles W. Gorton and Dr. Jude T. Sommerfeld for taking time to review this work.

I am especially grateful to Ian Stenhouse, my advisor at the Loughborough University of Technology, England, and C. N. Davies for his correspondence with me.

I would also like to express my appreciation to the U. S. Environmental Protection Agency, a grant from which made the completion of this work possible.

Finally, my special thanks are extended to my wife, Charlene, for her assistance in typing the paper, her encouragement and sense of humor, all of which made life better during the writing of this paper.

TABLE OF CONTENTS

LIST OF TABLES

LIST OF FIGURES

NOMENCLATURE

a	Dimensionless factor defined on page 6
C	Number concentration
C_o	Initial uniform number concentration
d	Particle diameter
d_{max}	Largest diameter in range
$\bar{d}$	Mean particle diameter
D	Diffusion coefficient
g	Gravitational acceleration, 980 cm/s^2
k	Percent average Brownian motion that the mean size particle experienced during a sedimentation analysis.
K	Boltzmann's constant, $1.38 \times 10^{-16} \frac{g\ cm^2}{s^2 {}^oK}$
L	Total depth of the sedimentation cell
t	Time
t_f	Time required for a sedimentation analysis
t'	Dimensionless time
T	Temperature
v	Settling velocity
x	Depth
y	Dimensionless depth
α	Ratio of diffusional displacement to displacement due to settling
γ	Mean value of α in a sedimentation analysis
η	Fluid viscosity
$\Delta\rho$	Effective density of a particle in a fluid

SUMMARY

Sedimentation analyses based on Stokes' law provide a reliable method for the determination of particle size distributions. A lower limit of applicability is established by the equalizing nature of diffusion since Stokes' law assumes that the particles are settling only under the influence of field and drag forces. Although the mathematics describing settling and diffusing systems was developed more than 50 years ago, to date only the differential equation involved has been verified experimentally. The purpose of this investigation was to use various solutions to this differential equation to predict the theoretical effect of diffusion on a sedimentation analysis and to compare these results with experimental data.

Particles in the 1 to 0.1 micrometer range were employed. Electron micrographs were used to determine the actual particle size distributions. To enable comparison of results of different experiments, the ratio of Brownian motion to settling motion was established. A series solution best represented the experimental data over the range of values examined for this ratio. However, a much simpler equation can be used for approximation purposes within certain range limits.

It is concluded that the ratio of Brownian to settling motion can be employed as a guide for determining whether or not a sedimentation analysis is affected by diffusional forces. By changing defining parameters--for example, viscosity, effective density, or the time required for the analysis--to achieve an acceptable value for the ratio, an accurate size determination may be obtained.

CHAPTER I

INTRODUCTION

Gravity sedimentation techniques are commonly employed for determining the size distribution of particulate matter. Including use of the ultracentrifuge, these techniques are capable of measuring particles from 0.001 to 100 micrometers in diameter. A great variety of particles such as dusts found in industrial atmospheres, pollens, bacteria, viruses, combustion nuclei, and dust capable of respiratory tract damage, fall within this size range and may be measured by sedimentation techniques.

All sedimentation techniques, whether the settling force is gravitational or centrifugal in nature, are based upon Stokes' law which relates the particle terminal velocity to the physical characteristics of the particle-fluid system in which it is settling. Inherent in Stokes' law is the assumption that each particle is settling in an infinite medium with only field and drag forces acting on it. This generally places a lower limit on the application of sedimentation techniques since Brownian movement produces a diffusion force not accounted for by Stokes' law that tends to equalize the density distribution caused by settling. Even though diffusional motion influences all sedimentation analyses, the extent of its effect is not noticeable until the particle sedimentational displacement approaches its root mean square Brownian displacement. This research is concerned with a quantitative evaluation of sedimenting and diffusing systems in which the particles are measurably affected by both diffusion and gravity.

History

The theoretical treatment of the combined effect of diffusion and sedimentation of small particles has long been an area of interest for mathematicians and particle technologists since the discovery of Brownian motion. In 1894, Th. Des. Coudres (1) derived the partial differential equation that describes the time rate of increase in concentration as a function of the depth in a settling and diffusing system, namely

$$\frac{\partial C}{\partial t} = D \frac{\partial^2 C}{\partial x^2} - v \frac{\partial C}{\partial x} \qquad (1)$$

where C is the number concentration, D the diffusion constant, t time, v sedimentation velocity, and x the depth below the upper surface. As time goes to infinity, a steady state condition is approached and the concentration is easily resolved as an exponential function of depth. This condition of steady state was verified by Perrin (2) in 1916.

Smoluchowski (3), Mason and Weaver (4), and Davies (5) have published various solutions to equation (1). The main difference among the solutions is due to the choice of boundary conditions. Unfortunately, these solutions have never been of much practical value due to their complexity (most are in infinite series form) and, even when the necessary calculations of how the concentration should vary with time and depth were made, there was no experimental technique available with which to substantiate their validity. In 1957, Richardson and Wooding (6) verified equation (1) by observing monodisperse aerosols with optical equipment to monitor settling depth and concentration as time progressed. Equation (1) was approximated by finite differences, and reasonable agreement with

theory was obtained.

Solutions of Equation (1)

In order to solve equation (1) analytically, certain assumptions concerning boundary conditions are required. The boundaries usually chosen are t=0, x=0, and x=L, where L is the total depth of the container. Although initially (t=0) any particle distribution is possible, a uniform distribution yields easily to mathematical treatment and is the most common assumption since it can be achieved experimentally. The boundary conditions assumed at x=0 and x=L can be divided into two classes:

(1) All particles striking an enclosing interface presented by the container reflect back into the bulk of the fluid leaving the total number of particles in suspension constant. This assumption is usually employed at free surfaces such as the gas-liquid interface presented by the upper surface of a partially filled sedimentation vessel. Such an interface is referred to as a perfect reflector.

(2) All particles striking an enclosing interface stick to it and are thus eliminated from the suspension. This assumption is used in conjunction with either small particles that will stick to the wall instead of reflect or with liquid aerosols. Eventually all particles in a suspension enclosed by adsorbing walls will disappear, and the final bulk concentration will be zero. Such an interface is referred to as a perfect adsorber.

This research deals with three different solutions to equation (1): C. N. Davies' model which assumes the top and bottom of the sedimentation cell to be perfect adsorbers, Mason and Weaver's model which assumes top

and bottom to be perfect reflectors, and, finally, Berg's (7) approximation to an equation derived by Mason and Weaver describing an infinitely deep cell with a perfectly reflecting top. No combination of reflecting and adsorbing interfaces were considered since the upper and lower boundaries of the cell used experimentally were sufficiently removed from each other when compared to the particle sizes involved that the condition at one interface did not affect the condition at the other, and, therefore, a model that assumes an adsorbing top and reflecting bottom gives the same result in the type of sedimentation analysis with which this research is concerned as a model that assumes a perfectly adsorbing top and bottom.

CHAPTER II

THEORETICAL AND EXPERIMENTAL DISCUSSION

Mathematical Models of Settling and Diffusing Systems

For a complete derivation of the solutions to equation (1), previous references should be consulted. In this thesis, it will suffice to discuss only the assumptions employed in their derivations. The assumptions used by Davies to solve equation (1) were:

1. The vertical walls of the settling cell are too remote for diffusion toward them to have any effect on the concentration.

2. No particle-particle interactions are possible and hydrodynamic interference is negligible.

3. The suspending medium completely fills the entire sedimentation cell.

4. The settling cell consists of a perfectly adsorbing top and bottom.

5. The terminal velocity of the particles is determined by Stokes' law, and the diffusion coefficient obeys the Stokes-Einstein equation.

6. Initially, the particles are uniformly distributed throughout the sedimentation cell.

Davies' solution is given in two forms; one as eigen function expansions and a second as an integral solution* to the expansion for

*In the process of checking these two solutions, a printing error in the integral solution was uncovered. The two v's in the first group of equation 46, page 109 of the referenced article should be changed to u's. The correct arguments of the error functions in h_1 should be (2w+u) and (w+u).

the case when a is small. Since the upper limit of "small" was not specified, the series expansions were used in the form:

$$\frac{C}{C_o} = \exp\left(\frac{2y-t'}{4a}\right) \sum_{n=1}^{\infty} \frac{2\sin(n\pi y)(1-(-1)^n \exp(-1/2a))\exp(-an^2\pi^2 t')}{n\pi(1+1/4a^2\pi^2 n^2)} \qquad (2)$$

where $y = x/L,$

$$t' = \frac{tg\Delta\rho d^2}{18L\eta} = tv/L,$$

and

$$a = \frac{6KT}{L\pi d^3 g\Delta\rho} = D/vL,$$

where C_o is the initial number concentration of particles with diameter d, g the gravitational acceleration, $\Delta\rho$ the density of the particle minus the density of the suspending fluid, d the particle diameter, η the fluid viscosity, K the Boltzmann's constant, and T the temperature.

Mason and Weaver's equation makes use of the same basic assumptions as for equation (2) such as neglecting wall effects, no particle-particle interaction or hydrodynamic effects, Stokes' settling velocity, and initial uniform concentration. In addition, it was assumed that the suspending liquid only partially fills the container, i.e., the upper interface is gas-liquid, and that the upper and lower surfaces are perfect reflectors.

This solution is also given in two forms; a series form and an integral form for small values of a. Once again, the series solution was used in the form:

$$\frac{C}{C_o} = \frac{\exp(y/a)}{a(\exp(1/a)-1)} + 16a^2\pi\exp\left(\frac{2y-t'}{4a}\right)$$

$$\sum_{n=1}^{\infty} \frac{\exp(-an^2\pi^2t')n(1+(-1)^{-n}\exp(-1/2a))(\sin(n\pi y)+2\pi n\cos(n\pi y))}{(1+4\pi^2n^2a^2)^2} \qquad (3)$$

where C_o, y, t', and a are as used in equation (2).

On physical grounds it would be expected that this equation and Davies' equation would approach one another for small values of the diffusion coefficient, since, with large particles, there is very little diffusional motion and whether the upper surface reflects or adsorbs incident particles would be of no consequence because for this situation no particles would strike the upper surface.

In the same paper that Mason and Weaver presented the previous equation, there appeared the equation

$$\frac{C}{C_o} = v\sqrt{t/D\pi}\ \exp\left[\frac{-(vt-x)^2}{4Dt}\right] + 1/2\left[1-\operatorname{erf}\left(\frac{vt-x}{\sqrt{4Dt}}\right)\right] +$$

$$\tfrac{1}{2}\exp(vx/D)\left[1+\frac{v}{D}(vt+x)\right]\left[1-\operatorname{erf}\left(\frac{vt+x}{\sqrt{4Dt}}\right)\right] \qquad (4)$$

which contains all the assumptions of equation (3) in addition to assuming that the suspending fluid is infinite in depth. It was intended to approximate equation (3). Berg used equation (4) and assumed that the first and third terms cancel to obtain equation (5)

$$\frac{C}{C_o} = \tfrac{1}{2}\left[1-\text{erf}\left(\frac{vt-x}{\sqrt{4Dt}}\right)\right]. \qquad (5)$$

In order for these two terms to cancel one another, the particle concentration in the upper portion of the suspension must be zero. Thus equation (5) would be expected to be valid for large particles with small diffusion coefficients. Since in this research the depth of the settling cell was much greater (by a factor of 35,000) than particle diameters, equation (5) would be expected to equal equations (3) and (2) for large particles because the lower boundary condition should not affect the upper boundary condition.

Sedimentation Analysis of a Settling and Diffusion Suspension

The influence of diffusion on a sedimentation analysis may be illustrated by considering a suspension of monodisperse particles with diameter d in a container. Prior to t=0, concentration uniformity is maintained by agitation. At t=0, the agitation is stopped and eddy currents dissipate. If the particle-fluid characteristics are within Stokes' regime, then all the particles will begin to fall vertically with the same characteristic terminal velocity. After a certain length of time, a definite interface will be observed in the upper portion of the suspension between pure liquid (above) and suspended particles (below). Sedimentation analysis of such a system will show a size distribution such as Curve A of Figure 1. If, however, the particles are small enough to be affected by diffusional as well as gravitational forces, then all the particles will not fall vertically. While some particles are settling according to Stokes' law, other particles are forced in random directions by molecular bombardment.

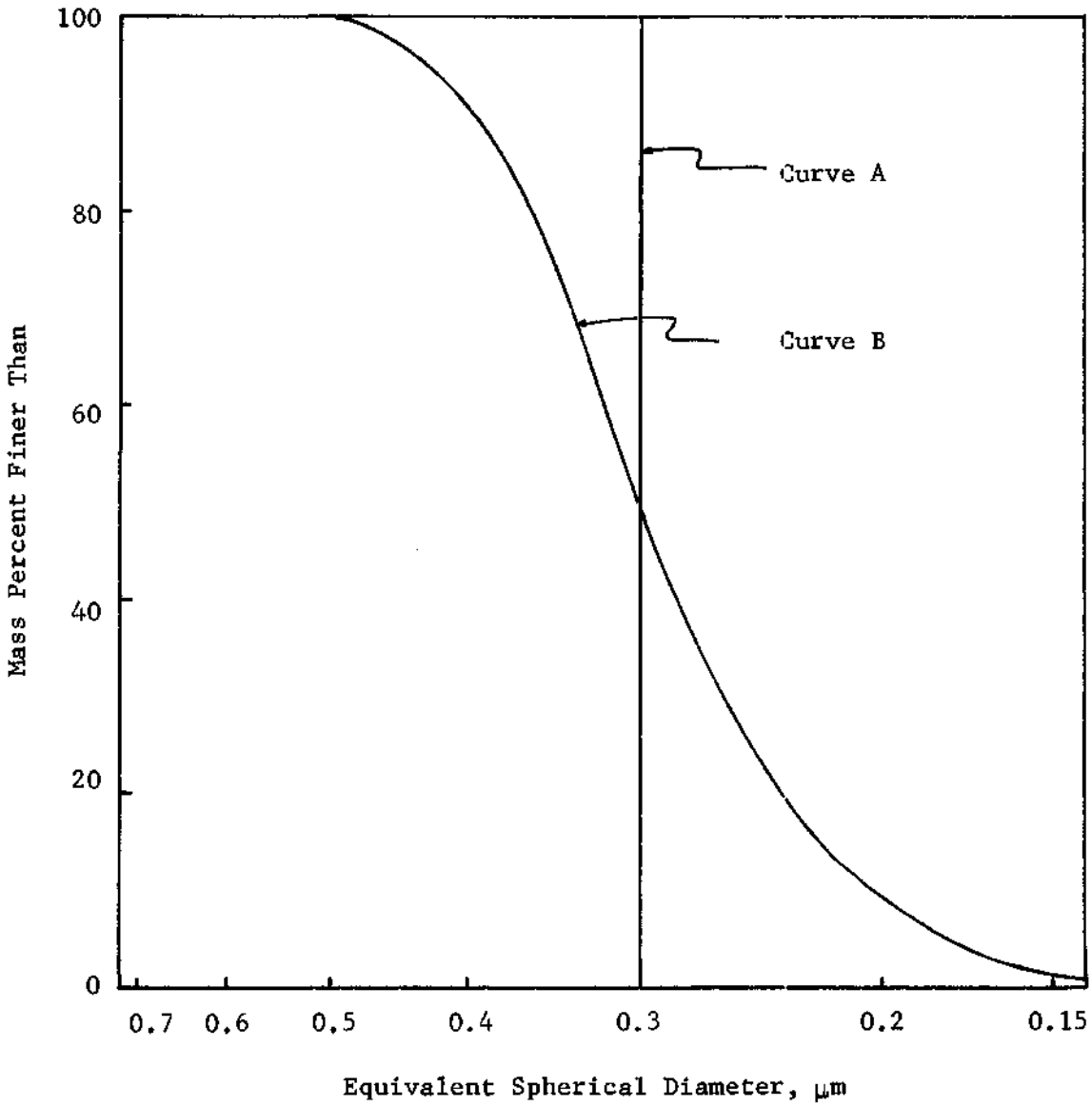

Figure 1. The Expected Effect (Curve B) of Diffusion on a Sedimentation Size Analysis of Monodisperse (0.3μm) Particles (Curve A)

This causes the previously well-defined interface considered above to become clouded and spread over a small region above and below the interface. Sedimentation analysis in this situation will show an erroneous size distribution such as Curve B in Figure 1 because the particles are being knocked about and do not always settle according to Stokes' law.

The amount of spreading of the actual size distribution in Figure 1 caused by diffusion depends mainly upon particle and fluid characteristics. In general, the smaller the particles, the greater the spreading. However, for a distribution with sizes ranging from 10 micrometers down, a sedimentation analysis in water will not be measurably influenced by diffusion since, even though the 0.5 to 0.1 micrometer particles diffuse, they contribute very little to the total mass of the particles.

To determine whether or not a sedimentation analysis was measureably influenced by diffusion, the ratio (α) of the root mean square displacement of the mean size particle in the distribution along an axis due to diffusional motion to the displacement of the same particle due to settling was considered. In quantitative terms, this ratio is

$$\alpha = \frac{\sqrt{2KTt}}{\frac{\Delta\rho g d^2 t}{18\eta}} = \frac{18}{\Delta\rho g d^{5/2}} \sqrt{\frac{2KT\eta}{3\pi t}} . \qquad (6)$$

For a given sedimentation analysis, α is a function of d and t. In order to find the average value of α for the analysis, the mean of α as a function of d and t could be found. However, as shown in Figure 1, the true size distribution is unknown if diffusion influences the analysis. Since the effect of diffusion is more noticeable in the analysis of a monodisperse

as compared to a polydisperse suspension, the most conservative assumption is that the particles under consideration are monodisperse with a diameter $\bar{d}$ equal to the mean diameter obtained from the sedimentation analysis. With a monodisperse distribution, this approach is accurate, while with a polydisperse distribution, it over-estimates the true value of γ. By replacing d in equation (6) with $\bar{d}$ and integrating α over the time required for a sedimentation analysis and then dividing by the elapsed time of the analysis, the mean value of α, defined as γ, for the size analysis can be calculated. That is, γ becomes

$$\gamma = \frac{36}{\Delta\rho g \bar{d}^{5/2}} \sqrt{\frac{2KT\eta}{3\pi t_f}} \tag{7}$$

where t_f is the time required for the sedimentation analysis. When γ is converted to a percentage of the total motion, it may be interpreted as the percent average Brownian motion that the mean size particle in the suspension experienced during the sedimentation analysis.

According to equation (7), little settling should be detected for large values of γ since diffusional displacement would be much greater than sedimentational displacement. Thus small values of γ are required for reliable sedimentation analyses. By studying the effect of diffusion on several sedimentation analyses and comparing the calculated value of γ for each experiment, some idea of the maximum allowable value of γ for valid results should be obtained.

Description of Instrumentation

Since the mechanism of diffusion is the same in a liquid as it is

in gas, the choice of the suspending fluid is one of convenience. Liquid rather than air was used as the suspending medium in the experimental portion of this study since in a liquid there is no slip between particles and molecules and thus no need to know the mean free path of the fluid or to rely on slip correction factors.

The sedimentation analyses in this research were accomplished with a commercial, Model 5000, Particle Size Analyser* which uses a finely collimated (0.0051 centimeter vertical thickness) x-ray beam to measure particle concentration in terms of the absorbence of a deflocculated suspension relative to the suspending fluid. Due to the mass interaction of x-rays, the transmittance of the x-ray beam is inversely related to the weight concentration of suspended particles in the beam path. By measuring the transmittance of the suspension at various sedimentation depths as a function of time and then electronically analysing this signal to yield the ratio of local concentration to initial concentration, a plot of "Cumulative Mass Percent Finer" as a function of "Equivalent Spherical Diameter" (calculated from Stokes' law by an internal computer) is drawn on an x-y recorder. It is inherent in Stokes' law that the settling velocity is directly proportional to the square of the particle diameter. Thus very small particles have extremely slow settling rates and an analysis of a distribution containing very fine particles can be extremely time consuming. In order to minimize the time required for an analysis, the distance between the beam and the top of the cell is continuously decreased in the instrument so that the sedimentation depth is inversely related to

*Micromeritics Instrument Corporation, Norcross, Georgia

settling time. This distance and the elapsed time form the basis of the Stokes' law calculation.

Several pertinent features of this analyser with respect to theoretical simulation are:

1. The cell is thermostatically controlled by cartridge heaters to within $\pm 0.5^{\circ}K$, thus minimizing convection currents caused by thermal gradients.

2. The sedimentation cell has a depth of 3.49 centimeters and a rectangular base 1.27 x 0.315 centimeters.

3. Prior to a size analysis, the particle density and fluid viscosity are programmed into the instrument for the Stokes' law calculation in the form of a rate constant which determines the time required for the analysis.

4. Before an analysis, the suspension is continuously pumped through the cell to assure initially a uniformly distributed bulk concentration.

5. At the moment of initiating an analysis, the cell is automatically sealed and a programmed time delay based on the rate constant is allowed for the dissipation of all eddy currents.

6. During an analysis, the sedimentation cell is completely filled with the sample suspension (suggesting a perfectly adsorbing top as assumed in Davies' solution to equation (1)).

7. The cell continuously moves downward according to a preset program based on the rate constant, the movement being controlled by stepping motors.

8. The electrical and mechanical variables are said to contribute errors less than ± 1.0 percent (8).

9. Due to the fine collimation of the x-ray beam, a particle 0.2 micrometer in diameter can be measured to within ± 0.05 micrometer.

Theoretical Simulation

In order to compare theory with experiment, the x-ray sedimentation analyser was completely simulated on a computer using the three previously described diffusion-sedimentation models, equations (2), (3), and (5). This method of comparison simplified presentation of the results, allowed for the comparison at every point of the experimental curve, and helped in determining what effect various changes in experimental techniques would have on a sedimentation analysis.

The method used to compare theory with experiment was first to obtain the actual equivalent size distribution, on a mass basis, of the particles comprising the suspension. This was obtained by counting particles from electron micrographs with a Zeiss Particle Size Counter, Model TGZ3. The distribution was then broken down into n steps or groups of monodisperse particles. A value of settling time t was chosen and, by knowing the distance x that the x-ray beam was from the upper interface at time t for a particular experiment, a model could be selected to calculate the particle concentration of each monosize group at the chosen time and depth. Each of these n concentrations was then multiplied by the mass fraction represented by the group. The sum of these n products was taken to be the total mass fraction of particles at depth x and time t and should be equal to the relative concentration encountered by the x-ray beam corresponding to a particle characterized by a settling velocity of x/t. A sample calculation of this nature is presented in Appendix B. By

choosing several time-depth pairs, the complete theoretical size analysis was drawn. Providing all the assumptions used to derive each of the three theoretical models were valid and the actual size distribution used in the simulation was correct, the result should coincide with the size distribution obtained from the Model 5000 instrument.

CHAPTER III

DISCUSSION OF RESULTS

The size distribution obtained from electron micrographs (A curves) and hereafter assumed to be the true distribution, the theoretical influence of diffusion on the sedimentation analysis (B curves), and the sedimentation analysis given by the sedimentation instrument (C curves) are shown in Figures 2-8. With respect to the B curves, B1 was calculated using Davies' solution, equation (2); B2 is Mason and Weaver's equation (equation (3); and B3 is Berg's result, equation (5). Table 1 shows the value of γ and the corresponding percent Brownian motion, defined as k, for each experiment.

The experimental error in the A and B curves of the first two figures resulted from using a small sample size to determine the actual partical distribution. In Figures 4-8, the experimental error in the C curves resulted from having to use low volume concentrations in the sedimentation analysis. In contrast to the Fe_2O_3 and silver halide samples, the SiO_2 particles used in these experiments were spherical and easily dispersed for electron micrograph purposes. It was therefore possible to determine the SiO_2, Lots I and II, A curves with considerable accuracy. Appendix C should be consulted for a more thorough description of the experimental errors.

Within experimental error, agreement between theory and experiment is good with the exception of the Lot II, experiments 1 and 2. Lot II,

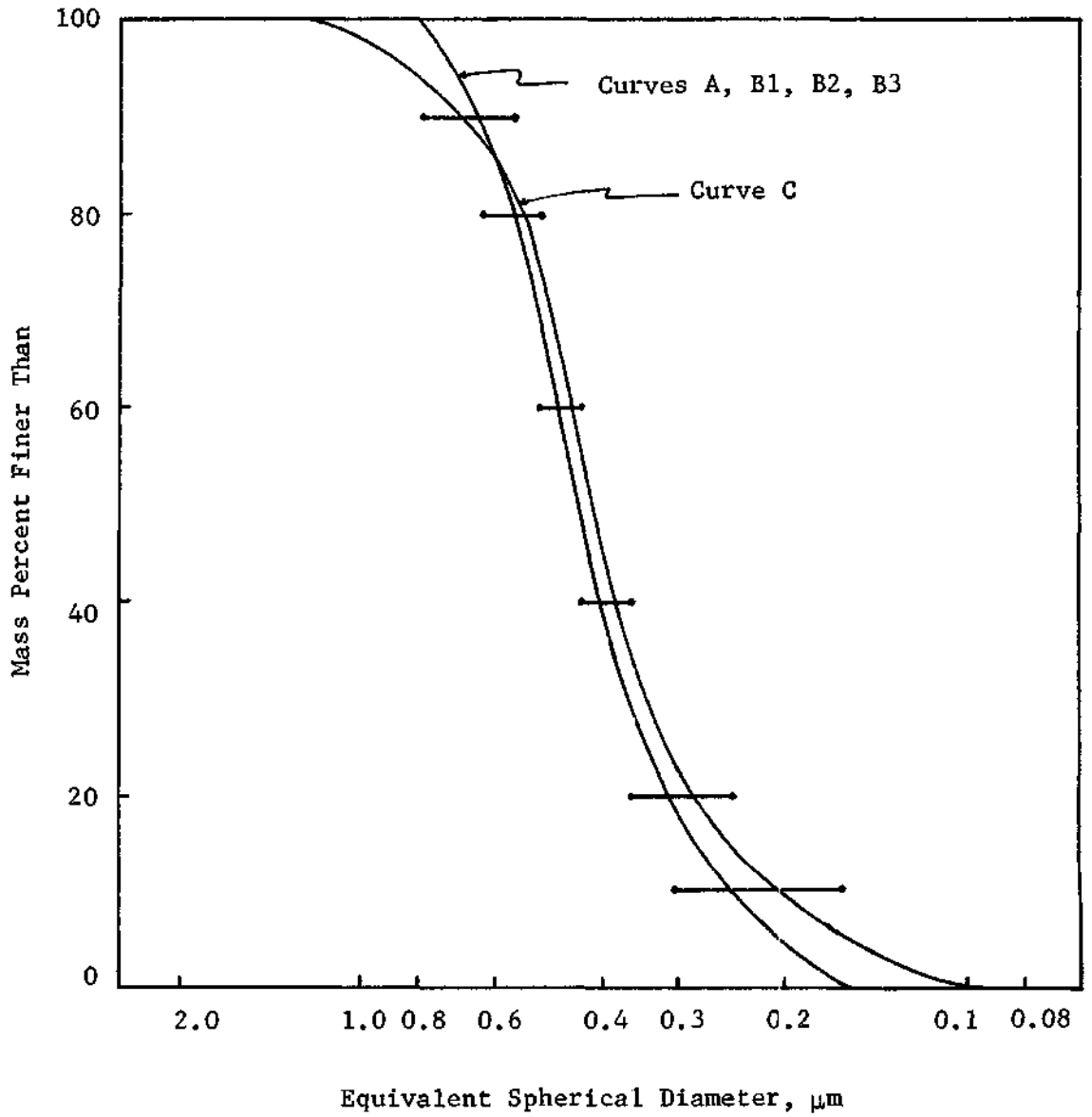

Figure 2. Comparison Between the Electron Microscope (Curve A), Predicted (Curve B), and Experimental (Curve C) Size Analyses for Fe_2O_3 (Mapico Red) Sample Showing Experimental Limits

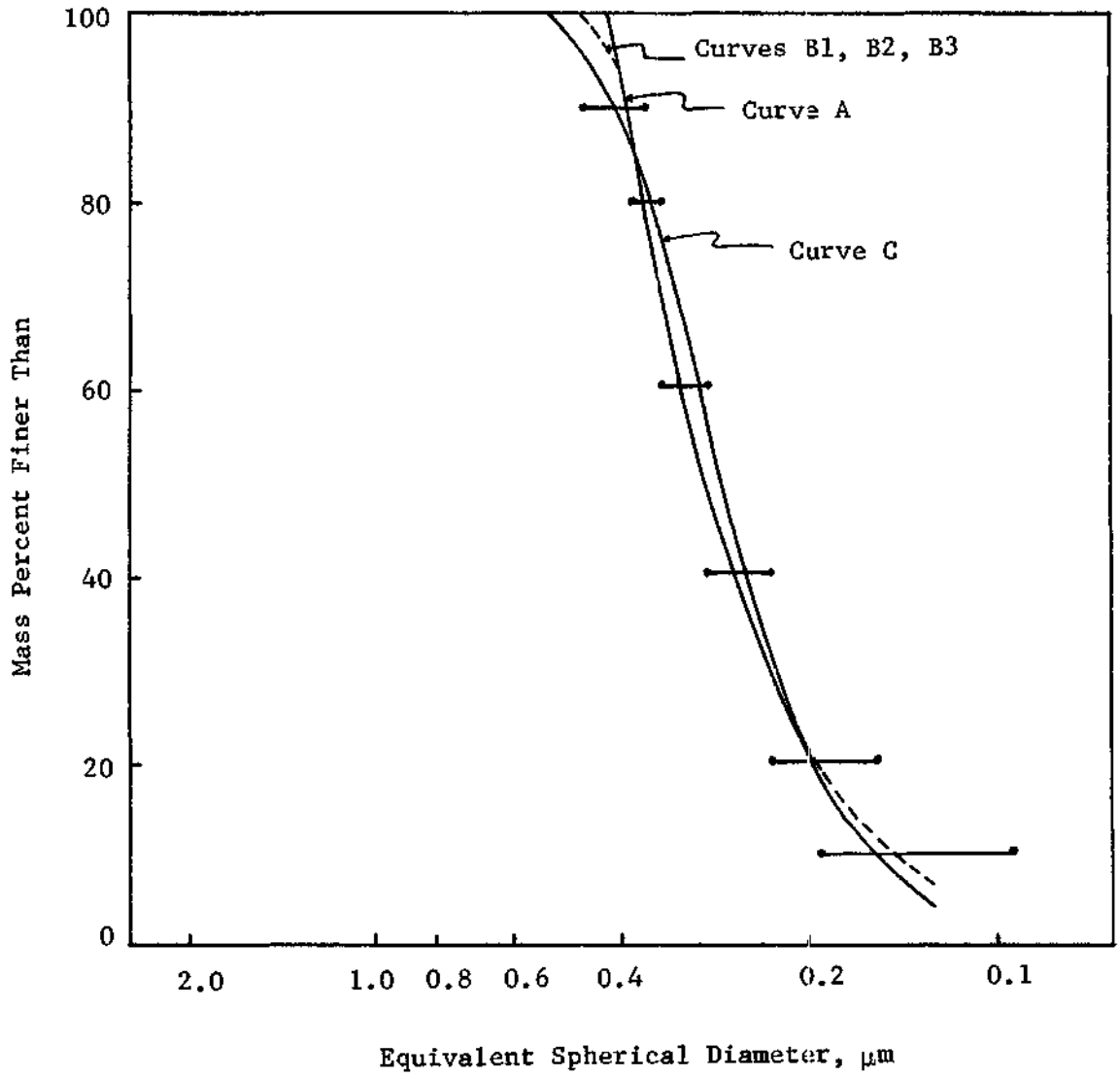

Figure 3. The Effect of Diffusion on a Sedimentation Analysis of Silver Halide

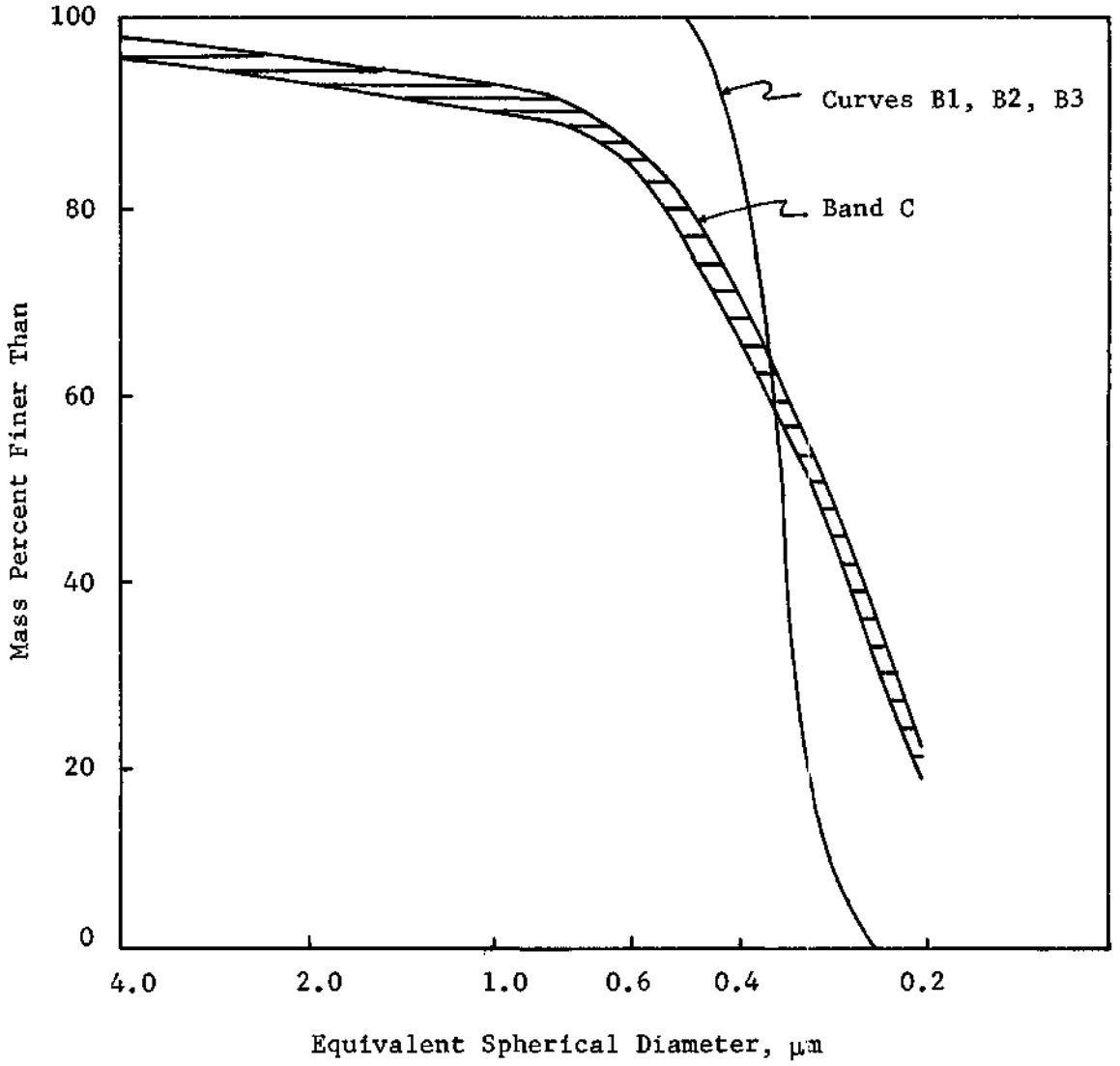

Figure 4. Sedimentation Analysis of SiO_2, Lot II, Exhibiting Agglomeration and Diffusion

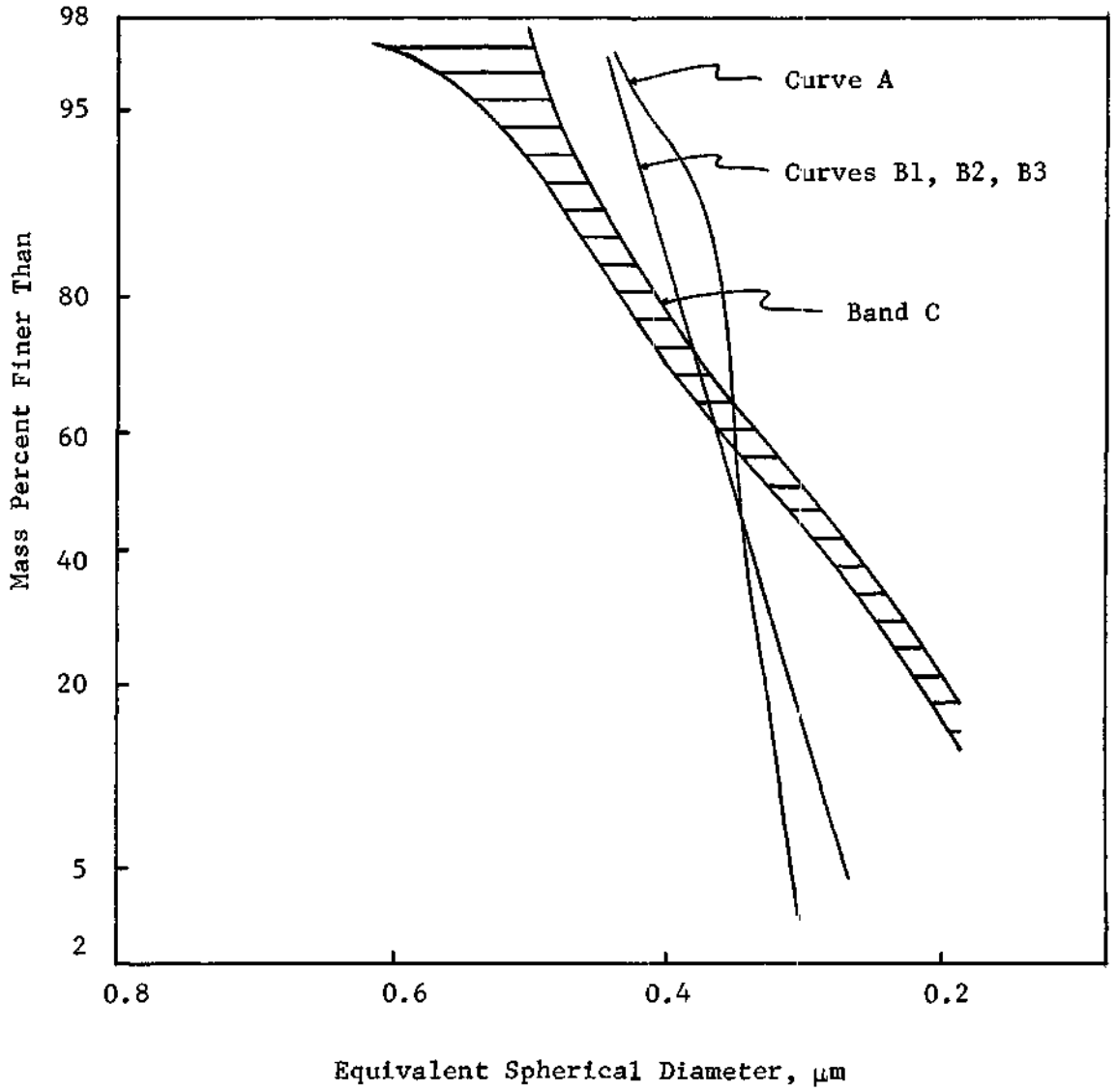

Figure 5. Sedimentation Analysis of SiO_2, Lot II, After Dispersing With a Sonic Bath. Concentration is 3.6 Volume Percent.

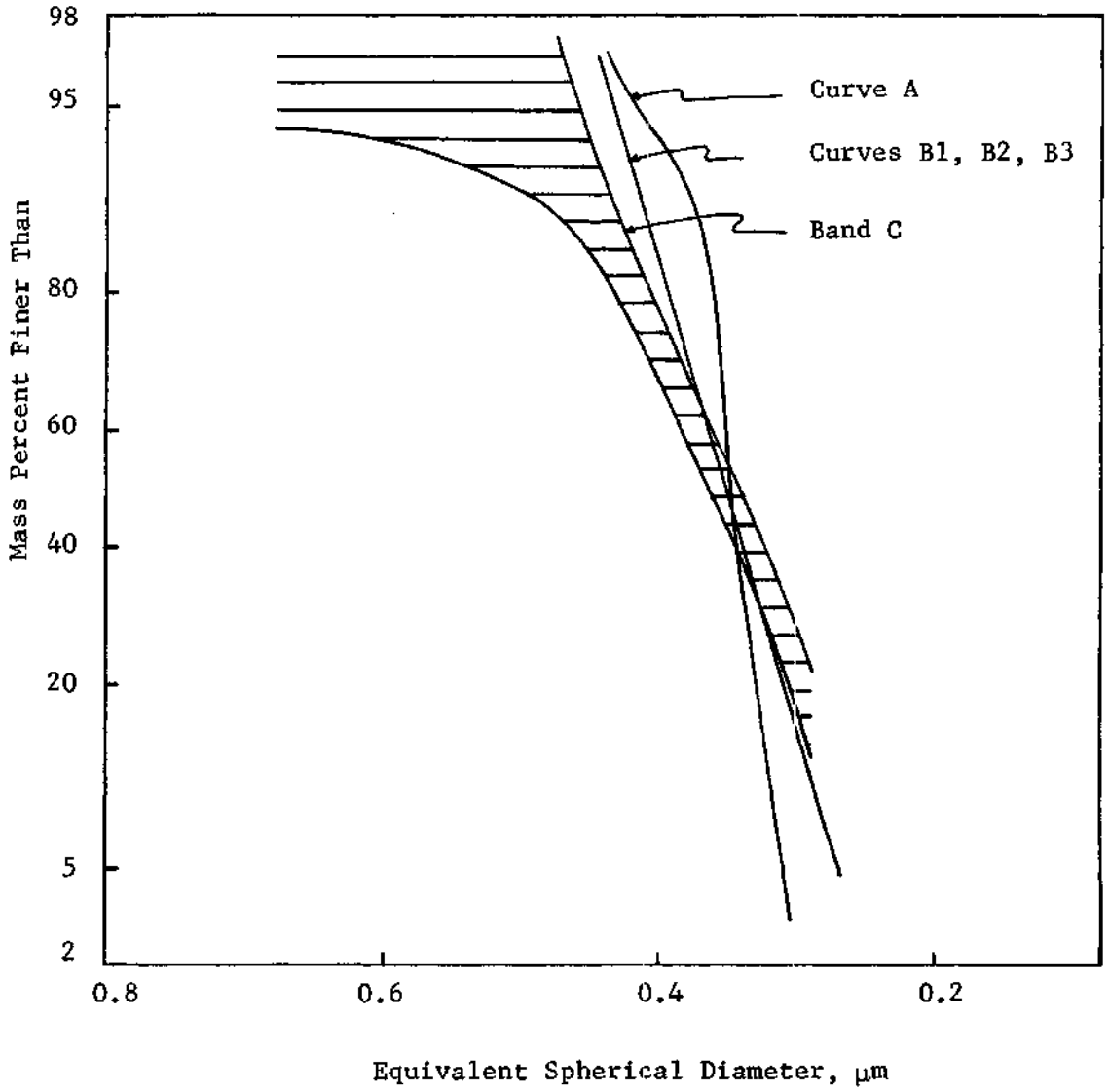

Figure 6. Sedimentation Analysis of SiO_2, Lot II, at a Volume Concentration of 1.8 Percent

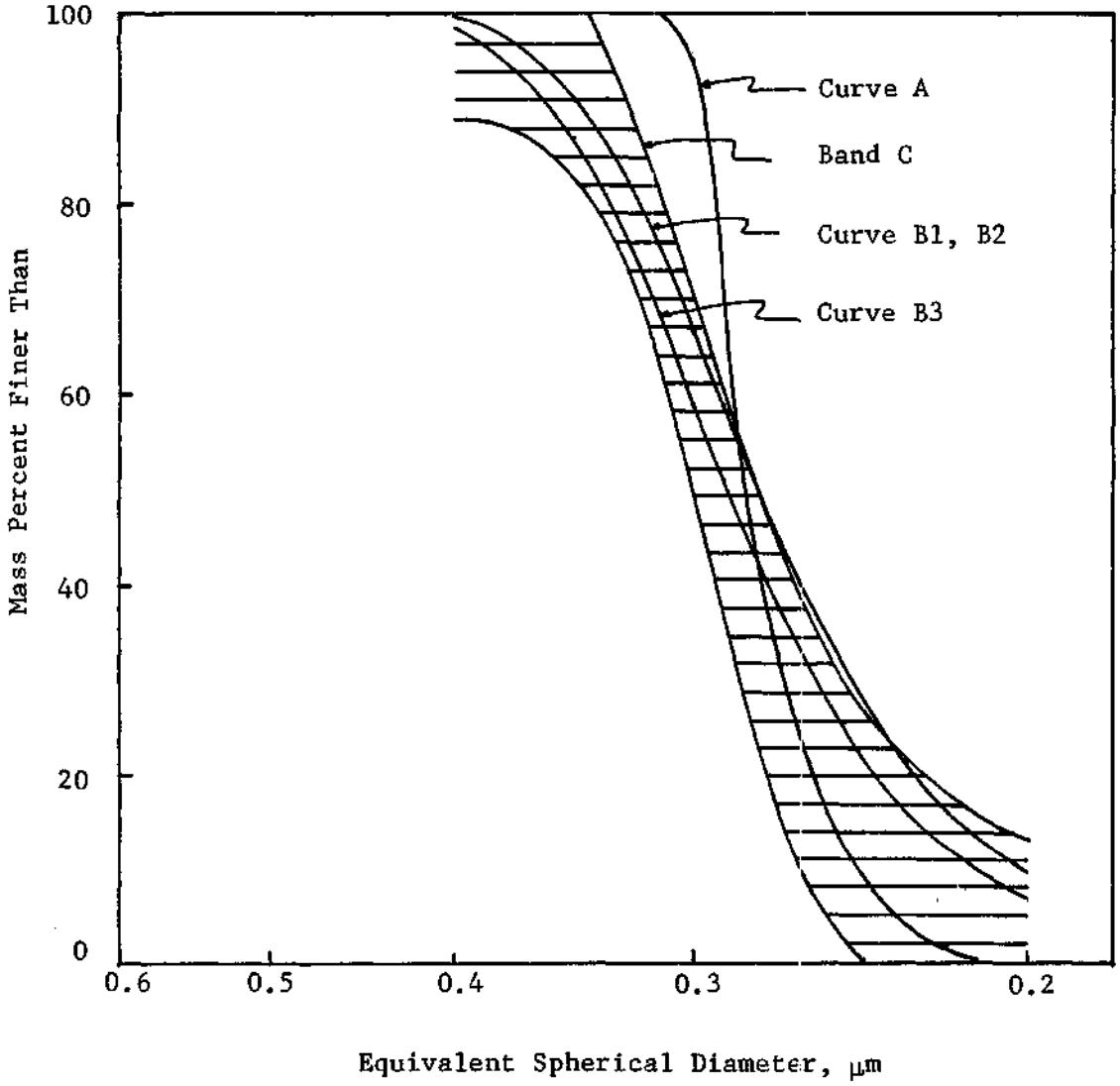

Figure 7. The Effect of Diffusion on the Sedimentation Analysis of SiO_2, Lot I, at a Volume Concentration of 1.1 Percent

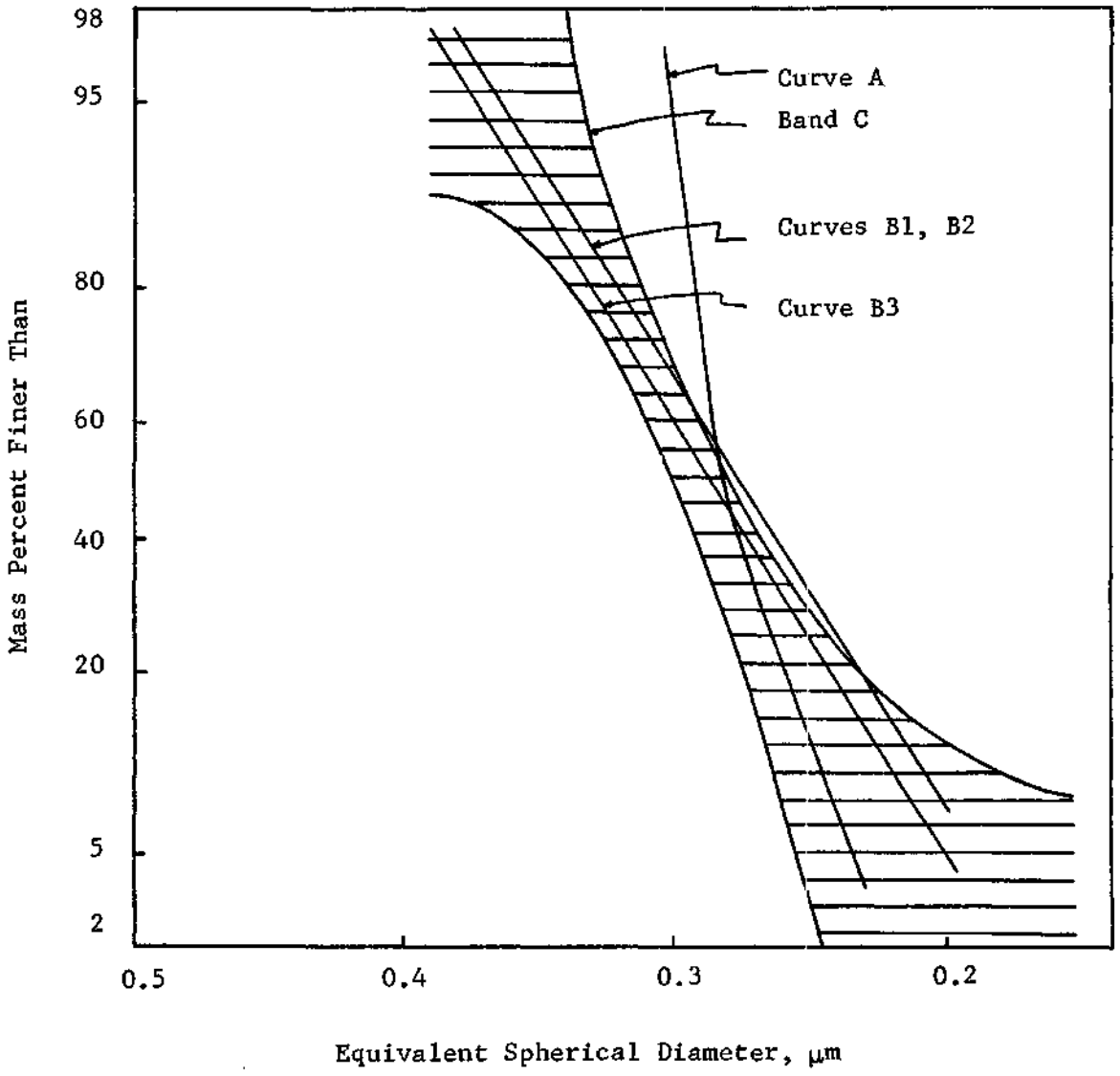

Figure 8. Replot of Figure 7 on Probability Grid

Table 1. The Mean Brownian Motion in Each Experiment

Sample	Figure	γ	Percent Brownian Motion, $k = 100 \times \frac{\gamma}{\gamma+1}$
Fe_2O_3	2	0.076	7.12
Silver Halide	3	0.24	19.3
SiO_2 Lot II	4-6	0.336	25.2
SiO_2 Lot I	7-8	0.579	35.7

experiment 3, reveals the source of error in the two previous experiments as being due to the formation of agglomerates and concentration effects.

Agglomeration results when particles collide and adhere to one another. If enough of these agglomerates are formed, the size analysis can be significantly in error. The size analysis in Figure 5 was made using Lot II particles that had been dispersed in a sonic bath. The size analysis in Figure 6 was made after diluting the Lot II, experiment 2, suspension from 3.6 volume percent to 1.8 volume percent. The size analysis of Lot I particles was conducted at a volume concentration of 1.1 percent in order to avoid concentration effects.

Figures 5, 6, and 8 are drawn using a probability scale in order to show that the theoretical result of diffusion on a sedimentation analysis is to distribute the particles in a manner such that a normal distribution results.

The fact that the various solutions to equation (1) do not differ significantly, except in the case where there was 35.7 percent Brownian motion (Lot I), implies that for values of γ less than about 0.3, a negligibly small proportion of particles strike the upper surface; for values of γ near 0.6 and larger, a significant number of particles that strike the interface adhere to it. Throughout all the experiments, Berg's equation closely approximates Mason and Weaver's series solution.

The results obtained not only shed light on the conditions existing at the interface, but provide a quantitative measure (γ) for determining whether or not diffusion influences a sedimentation analysis.

CHAPTER IV

CONCLUSIONS

The conclusions resulting from this work are summarized as follows:

1. Sedimentation analysis is an accurate and quick method for measuring size distribution providing diffusion and concentration effects do not influence significantly the motion of the particles.

2. Diffusion can easily invalidate a sedimentation analysis, the amount of disturbance introduced being inversely proportional to the square root of the time required for the analysis. The ratio of diffusional motion to sedimentational motion (γ) should be less than about 0.24 for a reliable size analysis using any sedimentation technique. By changing values defining this relationship such as viscosity, effective density, gravitational acceleration, or the time required for the analysis, an accurate size determination may be obtained.

3. In the closed system investigated, particles exhibiting slight diffusional motion do not significantly interact with the upper interface, while particles experiencing a large amount of diffusional motion tend to adhere to the walls.

4. For the purposes of approximating the effect of diffusion on a sedimentation analysis to within 5 percent, equation (5) is the best of the three equations considered due to its simplicity. However, once diffusion accounts for more than 30 percent of the motion, new boundary conditions must be considered and the appropriate model chosen.

APPENDICES

APPENDIX A

ELECTRON MICROSCOPE DATA

The following tables show the diameter distribution on a mass basis of the particulate systems used in the experimental section. The mapico red and silver halide data were obtained from reference (9). The SiO_2 distributions were obtained by measuring n particles from electron micrographs using the Zeiss Particle Size Counter, Model TGZ3, and converting from a count basis to a weight basis by using moments. The tables show the size intervals and mean size of each interval, the number of particles in each interval, and the mass fraction occupied by each interval for each particulate system.

Table 2. Mapico Red Distribution According to Electron Micrographs

Largest Diameter in Range d_{max}, μm	Mean Diameter in Range $\bar{d}$, μm	Number of Particles	Weight Fraction	Percent by Weight Less Than d_{max}
0.09	0.05	32	0.0030	0.30
0.19	0.14	33	0.0287	3.17
0.29	0.24	40	0.1237	15.54
0.39	0.34	28	0.2107	36.61
0.49	0.44	17	0.2537	61.98
0.59	0.54	9	0.2344	85.42
0.69	0.64	2	0.0833	93.75
0.79	0.74	1	0.0625	100.00
		Total: 167		

Table 3. Silver Halide Distribution According to Electron Micrographs

Largest Diameter in Range d_{max}, μm	Mean Diameter in Range $\bar{d}$, μm	Number of Particles	Weight Fraction	Percent by Weight Less Than d_{max}
0.04	0.02	25	0.001	0.1
0.08	0.06	26	0.009	1.0
0.13	0.105	27	0.040	5.0
0.17	0.15	28	0.094	14.4
0.21	0.19	16	0.101	24.5
0.25	0.23	13	0.138	38.3
0.29	0.27	7	0.117	50.0
0.34	0.315	6	0.161	66.1
0.38	0.36	5	0.187	84.8
0.42	0.40	3	0.151	99.9
	Total:	156		

Table 4. SiO_2, Lot I, Distribution According to Electron Micrographs

Largest Diameter in Range d_{max}, μm	Mean Diameter in Range $\bar{d}$, μm	Number of Particles	Weight Fraction	Percent by Weight Less Than d_{max}
0.19	0.185	1	0.0003	0.03
0.20	0.195	3	0.0011	0.14
0.21	0.205	15	0.0064	0.78
0.22	0.215	25	0.0123	2.01
0.23	0.225	35	0.0198	3.99
0.24	0.235	60	0.0388	7.87
0.25	0.245	78	0.0573	13.60
0.26	0.255	97	0.0806	21.66
0.27	0.265	120	0.1121	32.87
0.28	0.275	142	0.1486	47.73
0.29	0.285	242	0.2824	75.97
0.30	0.295	150	0.1945	95.42
0.31	0.305	32	0.0459	100.00
	Total:	1000		

Table 5. SiO_2, Lot II, Distribution According to Electron Micrographs

Largest Diameter in Range d_{max}, μm	Mean Diameter in Range $\bar{d}$, μm	Number of Particles	Weight Fraction	Percent by Weight Less Than d_{max}
0.29	0.285	13	0.0051	0.51
0.30	0.295	47	0.0203	2.54
0.31	0.305	65	0.0309	5.63
0.32	0.315	219	0.1146	17.09
0.33	0.325	124	0.0712	24.21
0.34	0.335	215	0.1349	37.70
0.35	0.345	408	0.2793	65.63
0.36	0.355	239	0.1781	83.44
0.37	0.365	13	0.0105	84.49
0.38	0.375	83	0.0727	91.76
0.39	0.385	19	0.0180	93.56
0.40	0.395	6	0.0061	94.17
0.41	0.405	0	0.0	94.17
0.42	0.415	12	0.0142	95.59
0.43	0.425	9	0.0114	96.73
0.44	0.435	7	0.0114	97.68
0.45	0.445	2	0.0029	97.97
0.46	0.455	13	0.0202	99.99
	Total:	1494		

APPENDIX B

CALCULATED DATA

The following tables present the calculated data used in preparing the B curves in Figures 2-8. When the calculated values of equations (2) and (3) are not given (represented by a dash), it is meant that the equation did not converge in the first 6000 terms of the series. In these cases, a sufficient number of concentrations were calculated using each equation to insure that equation (5) gave the same concentration as equations (2) and (3). Only the number of points necessary to draw the complete B curves were calculated.

Two simplifications were made in equations (2) and (3) due to limitations in the various computers* used for the simulation. Since the maximum value of a that occurred was 10^{-3} (Lot I experiment), the maximum value of exp(-1/2a) which appears in equation (2) was 10^{-217}. This factor was never calculated and was assumed to be zero. The same term appears in equation (3) and was neglected for the same reasen. Since y ranged from 0.005 to 0.1, the first term on the right-hand side of equation (3) had a maximum value of 10^{-388} and was also neglected in all calculations.

Table 6 illustrates how the three theoretical models were used to simulate the Model 5000. The three points calculated are for the SiO_2, Lot II, experiments (Table 9).

The histogram of the SiO_2, Lot II, particles was divided into 18

*Burroughs B5500, Univac 1108, and ICT 1905

discrete groups. By knowing the physical characteristics of the suspension and that at 63.5 minutes after initiating the experiment the x-ray beam was 0.0345 centimeters from the top of the cell, equations (2), (3), and (5) were evaluated for each of the 18 monodisperse groups. For example, each number shown in the third column represents the number fraction of particles according to equation (2) present at 63.5 minutes and at a depth of 0.0345 centimeters for a monodisperse suspension of particles with diameter $\overline{d}$ micrometers. Since the Model 5000 is based on mass concentration, each of the fractions in columns 3-5 was multiplied by the mass fraction that the corresponding mean diameter represented. The sum of each of the last three columns was then taken to represent the total relative mass concentration at the chosen depth and time. According to Stokes' law, for a particle to fall 0.0345 centimeters in 63.5 minutes in the given suspension, it is characterized by an equivalent diameter of 0.30 micrometer. Hence, according to equation (2), a sedimentation analysis should reveal that 13.3 percent of the particles on a mass basis are finer than 0.30 micrometer. Referring to Table 5, it is seen that in actual fact only 2.54 percent of the particles are finer than 0.30 micrometer. By choosing several time-depth pairs, the complete theoretical size analysis was drawn.

Table 6. Sample Calculations of the Theoretical Mass Concentration of Lot II Particles 63.5 Minutes After Initiating the Experiment for a Depth of 0.0345 Centimeters.

$\bar{d}$, μm	Mass Fraction	Equation: (2)	(3)	(5)	Mass Fraction x Equation: (2)	(3)	(5)
0.285	0.0051	0.5491	0.6175	0.6081	0.0028	0.0031	0.0031
0.295	0.0203	0.4694	0.5346	0.5276	0.0095	0.0109	0.0107
0.305	0.0309	0.3852	0.4448	0.4403	0.0119	0.0137	0.0136
0.315	0.1146	0.3009	0.3525	0.3504	0.0345	0.0404	0.0402
0.325	0.0712	0.2217	0.2635	0.2632	0.0158	0.0188	0.0187
0.335	0.1349	0.1523	0.1838	0.1847	0.0205	0.0248	0.0249
0.345	0.2793	0.0964	0.1182	0.1197	0.0269	0.0330	0.0334
0.355	0.1781	0.0555	0.0692	0.0706	0.0099	0.0123	0.0126
0.365	0.0105	0.0287	0.0363	0.0374	0.0003	0.0004	0.0004
0.375	0.0727	0.0131	0.0168	0.0175	0.0010	0.0012	0.0013
0.385	0.0180	0.0052	0.0068	0.0072	0.0001	0.0001	0.0001
0.395	0.0061	0.0018	0.0023	0.0025	0.0	0.0	0.0
0.405	0.0	0.0005	0.0007	0.0007	0.0	0.0	0.0
0.415	0.0142	0.0001	0.0002	0.0002	0.0	0.0	0.0
0.425	0.0114	0.0	0.0	0.0	0.0	0.0	0.0
0.435	0.0095	0.0	0.0	0.0	0.0	0.0	0.0
0.445	0.0029	0.0	0.0	0.0	0.0	0.0	0.0
0.455	0.0202	0.0	0.0	0.0	0.0	0.0	0.0
			Total Mass Fraction		≈ 0.1332	0.1587	0.1590

Table 7. Calculations of Curves B1, B2, and B3, Figure 2

Time, min.	Depth, cm	Equation: (2)	(3)	(5)	Stokes Diameter, μm
16.0	0.1494	--	--	94.0	0.73
20.8	0.116	--	--	84.3	0.56
41.6	0.058	14.6	14.9	14.6	0.28
66.5	0.0348	2.1	2.6	2.5	0.17

Table 8. Calculations of Curves B1, B2, and B3, Figure 3

Time, min.	Depth, cm	Equation (2)	(3)	(5)	Stokes Diameter, μm
17.0	0.737	--	--	99.8	0.446
18.3	0.0694	--	--	97.5	0.418
18.9	0.0663	--	--	92.5	0.401
19.7	0.0635	--	--	85.8	0.385
20.5	0.061	--	--	79.5	0.370
21.1	0.0595	--	--	75.2	0.360
21.6	0.0548	--	--	67.3	0.341
24.3	0.0515	--	--	56.6	0.312
26.7	0.0467	46.9	47.6	47.1	0.283
35.6	0.0351	23.1	25.2	24.8	0.213
42.7	0.0292	13.2	15.8	15.4	0.177
52.0	0.0242	7.1	9.8	9.3	0.146

Table 9. Calculations of Curves B1, B2, and B3, Figures 4-6

Time, min.	Depth, cm	Equation: (2)	(3)	(5)	Stokes Diameter, μm
42.6	0.0515	--	--	96.9	0.45
47.4	0.0465	--	--	86.7	0.40
50.2	0.0437	73.0	76.1	74.5	0.38
54.9	0.0398	45.7	49.9	49.0	0.34
57.8	0.0381	32.4	36.3	35.8	0.33
63.5	0.0345	13.3	15.9	15.9	0.30*
70.2	0.0312	4.3	5.5	5.6	0.27

*See Table 6 for this calculation

Table 10. Calculations of Curves B1, B2, and B3, Figures 7-8

Time, min.	Depth, cm	Equation: (2)	(3)	(5)	Stokes Diameter, μm
39.8	0.0468	98.8	99.5	99.1	0.405
46.5	0.04	87.0	90.5	89.8	0.346
53.9	0.0346	59.2	66.3	65.5	0.299
56.0	0.0333	51.0	58.5	57.8	0.288
69.6	0.0267	15.9	21.2	21.5	0.231
80.0	0.0231	6.14	9.07	9.51	0.199

APPENDIX C

EXPERIMENTAL DATA

In the collection of experimental data, four different particulate systems were studied: two SiO_2 samples (Lots I and II), Fe_2O_3 (mapico red), and silver halide. The following discussion and tables describe these particles, the experiments involving these particles, the results, and the error involved in the results.

Sample 1

The electron microscope and experimental data for the Fe_2O_3 and silver halide particles were obtained from an article written by Hendrix and Orr (8). Additional information concerning the physical characteristics of the analyses was obtained from the authors. In the size analysis of the mapico red sample by electron micrographs, 167 particles were counted which guaranteed the accuracy of Curve A with 99 percent assurance to within no less than 10 percent (9). The range of acceptable values drawn in Figure 2 are based on this error in Curves A and B. The small amount (7.1 percent) of Brownian motion was due mainly to the high density of the particles (See Table 11).

Sample 2

To determine the actual size distribution in the silver halide experiment, 156 particles were measured using electron micrographs. This guaranteed the accuracy of Curve A with 99 percent assurance to within 10 percent (10).

The range of acceptable values shown in Figure 3 are therefore based on this error in Curves A and B. In the sedimentation analysis, eight grams of silver halide gel were dispersed in 55 ml. of 0.05 percent Calgon solution (aqueous) and one drop of Kodak Photo-Flo 200 was added. The diffusion in this experiment was twice that in the Fe_2O_3 experiment even though the particles were more dense. This was due to the smaller mean diameter of the silver halide particles and the shorter time chosen for the analysis.

In Figure 3 the sedimentation curve is shifted to the left in order to compare the standard deviations of the various curves. The reason for considering only the variance and not the mean is that any error in the mean could be due to an error in the viscosity of the liquid or the relative density. An error in the relative density is suspected in this case since the silver halide particles were irregular and thus it was impossible to measure their effective settling density. An error of this type would only shift the curve in a horizontal manner parallel to itself without changing the standard deviation as long as the normal distribution is maintained.

Sample 3

The silicon dioxide particles used in the experiments were ideal for this type of analysis. SiO_2 spheres are precipitated when tetrapentyloxy silane reacts with water in the presence of ammonia (11). The suspension formed is very dilute (0.35 volume percent) and practically monodisperse. Figure 9 shows one of the electron micrographs used in the size determination of SiO_2, Lot II.

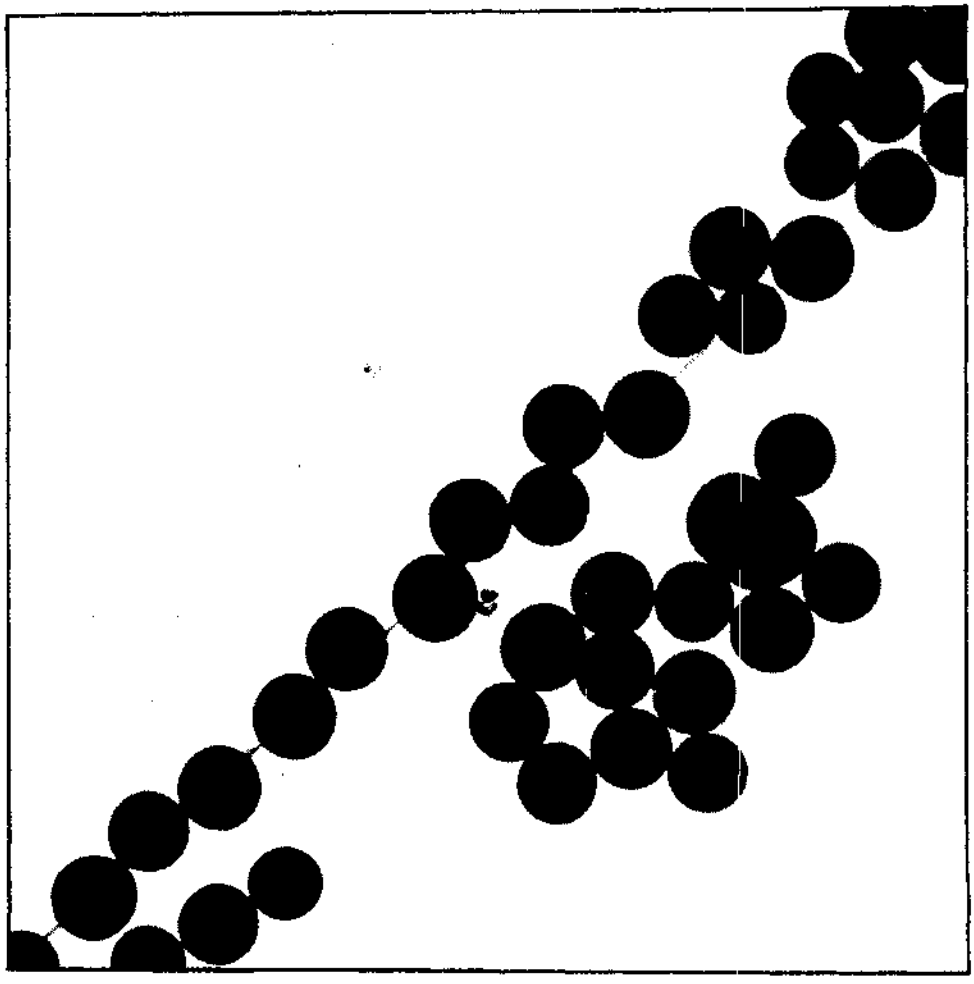

Figure 9. Electron Micrograph of SiO_2, Lot II, Particles. One Centimeter Equals 0.303 μm.

Although various alcohols may be used as the reaction medium, only ethanol was employed in these experiments. Lot I particles were removed from suspension by filtering and later dispersed in water for the size analysis. Several dispersing agents were used to prevent coagulation. In contrast to the previous two experiments, there is essentially no error involved in the A and B curves in Figures 7-8, since 1,000 particles were measured. The error in the analysis is due to error in the sedimentation curve. Since Stokes' law and Einstein's diffusion coefficient are valid only for infinitely dilute suspensions, a sedimentation analysis should be conducted at the lowest possible particle concentration. Unfortunately, SiO_2 is a low x-ray absorber, and relatively high concentrations (5.0 volume percent) were required to obtain full sensitivity from the Model 5000. Full sensitivity was therefore sacrificed for low concentrations, but a 1.0 percent (of full sensitivity) error was still encountered. The range encountered in the sedimentation analysis of Lot I particles was between 0 to 10 percent. In order to convert this to a 100 percent scale, each percent was divided by 0.1. For example, at 0.4 micrometer the range in "Cumulative Mass Percent Finer" was 8.9 to 11.0. On a 100 percent basis, this converts to 89.0 and 110 percent. These and similar values presented in Table 17 are shown as a band in Figures 7-8.

Sample 4

The SiO_2 Lot II particles were concentrated in the ethanol solution in which they were precipitated. The solution was stirred constantly by a magnetic stirrer while the ethanol was being evaporated at room temperature under a vacuum. Since 1,494 particles were measured (see Table 5),

virtually no error is involved in the determination of the A and B curves of Figures 4-6. As explained above, the error is due to the necessity of using low volume concentrations. The same suspension was used in the three sedimentation analyses of Lot II. The first analysis showed agglomeration and it was repeated after being dispersed in a sonic bath. The solution was then diluted with absolute ethanol and the sedimentation analysis was made a third time.

Table 11. Physical Characteristics of Each Sedimentation Analysis

System	Particle Density, g/cc	Liquid Density, g/cc	Viscosity, cp	Temp., °C	Elapsed Time, min.	k
Fe_2O_3	5.24	1.00	0.78	33	115.0	7.1
Silver Halide	6.00	1.00	0.75	33	59.6	19.3
SiO_2 Lot II	2.65	0.78	1.00	31	104.5	25.2
SiO_2 Lot I	2.65	1.00	0.75	33	88.7	35.7

Table 12. Sedimentation Analysis of Fe_2O_3

Equivalent Spherical Diameter, μm	Cumulative Mass Percent Finer*
1.3	100.0
0.9	96.0
0.7	91.1
0.6	86.0
0.5	73.0
0.4	45.5
0.3	22.7
0.2	10.2
0.15	4.9
0.10	0.5

*The error in each percent is ±1.0.

Table 13. Sedimentation Analysis of Silver Halide

Equivalent Spherical Diameter, μm	Cumulative Mass Percent Finer*
0.42	99.6
0.38	96.2
0.34	91.0
0.29	78.0
0.25	62.8
0.21	41.2
0.17	25.0
0.13	9.1

*The error in each percent is ± 1.0.

Table 14. Sedimentation Analysis of SiO_2, Lot II, Experiment 1

Equivalent Spherical Diameter, μm	Cumulative Mass Percent Finer Range	Range Converted to a 100% Scale
10.0	93.0 - 95.0	98.0 - 100.0
8.0	93.0 - 95.0	98.0 - 100.0
5.0	91.2 - 93.9	96.0 - 98.8
3.0	90.0 - 92.5	94.6 - 97.5
1.5	87.0 - 89.1	91.5 - 93.9
1.0	85.5 - 88.1	90.0 - 92.8
0.8	84.0 - 87.0	88.5 - 91.5
0.6	81.0 - 83.3	85.2 - 87.6
0.5	74.0 - 77.0	77.9 - 81.0
0.4	62.2 - 66.0	65.5 - 69.5
0.3	48.1 - 51.0	50.6 - 53.7
0.25	34.0 - 36.0	35.8 - 37.9
0.2	18.0 - 20.0	19.0 - 21.0

Table 15. Sedimentation Analysis of SiO_2, Lot II, Experiment 2

Equivalent Spherical Diameter, μm	Cumulative Mass Percent Finer Range	Range Converted to a 100% Scale
0.7	59.4 - 62.6	97.3 - 102.8
0.6	59.4 - 62.6	97.3 - 102.9
0.5	56.3 - 59.4	92.3 - 97.3
0.45	50.0 - 56.1	83.2 - 92.1
0.4	43.0 - 47.9	70.5 - 78.5
0.35	35.8 - 39.5	58.7 - 64.8
0.3	27.9 - 31.0	45.7 - 50.8
0.25	19.2 - 23.2	31.5 - 38.1
0.2	10.0 - 14.0	16.4 - 24.0
0.185	8.0 - 10.5	13.1 - 17.2

Table 16. Sedimentation Analysis of SiO_2, Lot II, Experiment 3

Equivalent Spherical Diameter, μm	Cumulative Mass Percent Finer Range	Range Converted to a 100% Scale
0.68	24.0 - 26.0	94.1 - 102.0
0.58	23.5 - 26.0	92.2 - 102.0
0.48	22.7 - 25.0	89.0 - 98.0
0.43	20.0 - 22.5	78.4 - 88.3
0.38	14.5 - 17.5	56.9 - 68.6
0.33	8.5 - 11.0	33.3 - 43.1
0.28	2.5 - 5.5	11.1 - 21.6

Table 17. Sedimentation Analysis of SiO_2, Lot I

Equivalent Spherical Diameter, μm	Cumulative Mass Percent Finer Range	Range Converted to a 100% Scale
0.5	8.9 - 12.0	89.0 - 120.0
0.45	8.9 - 12.0	89.0 - 120.0
0.4	8.9 - 11.0	89.0 - 117.0
0.35	8.4 - 10.3	84.0 - 103.0
0.3	5.1 - 7.1	51.0 - 71.0
0.25	0.3 - 3.1	3.0 - 30.0
0.2	-1.4 - 1.3	-14.0 - 13.0

BIBLIOGRAPHY

1. Coudres, Th. Des., Ann. Phys. und Chem., 52 (1894), 191-204.

2. Perrin, J. P., trans. by Hammick, D. L., Atoms, Constable, London (1923), 83-108.

3. Smoluchowski, M. von, Ann. Phys., 48 (1915), 1103-1112.

4. Mason, M. and Weaver, W., Phys. Rev., 2, 23 (1924), 412-426.

5. Davies, C. N., Proc. Roy. Soc., 200A (1949), 100-113.

6. Richardson, J. F. and Wooding, E. R., Chem. Eng. Sci., 7 (1957), 51-59.

7. Berg, S., Symp. on Particle Size Measurement, ASTM Spec. Tech. Publ. No. 234 (1958), 143-171

8. Oliver, J. P., Hickin, G. K., and Orr, C., Powder Technol., 4 (1970/71), 257-263.

9. Hendrix, W. and Orr, C., Second Particle Size Analysis Conference Bradford, England (1970), 133-146.

10. Montgomery, D., Rubber Age, 5, 94 (1964), 759-761.

11. Stober, W., Fink, A., and Bohn, E., J. Coll. & Interface Sci., 26 (1968), 62-69.